The Astrophysical Journal, 889:67 (7pp), 2020 January 20 https://doi.org/10.3847/1538-4357/ab60a1

Condensation of Atomic Carbon: Possible Routes toward Glycine

Serge A. Krasnokutski[1], Cornelia Jäger[1], and Thomas Henning[2]
[1] Laboratory Astrophysics Group of the MPI for Astronomy at the University of Jena, Helmholtzweg 3, D-07743 Jena, Germany; sergiy.krasnokutskiy@uni-jena.de
[2] Max-Planck Institute for Astronomy, Königstuhl 17, D-69117 Heidelberg, Germany
Received 2019 August 22; revised 2019 December 4; accepted 2019 December 9; published 2020 January 27

Abstract

Many organic molecules including amino acids and nucleobases are expected to be formed in astrophysical environments. In this article, we used both experimental and computational approaches to test the possibility of the glycine formation in the interstellar medium via C atom addition to ice mantels of dust particles. The reactions of C atoms with NH_3 and H_2 were studied experimentally. These reactions are found to be highly exothermic and barrierless, leading to the formation of the products CH_2NH and HCH. These product molecules are formed in excited states and therefore could immediately take part even in chemical reactions with energy barriers. The CH_2NH molecule is formed in the long-lived triplet state, which is above the most energetically favorable singlet state of about 20,918 cm^{-1} (~250 kJ mol^{-1}). Therefore, based on the results of quantum chemical computations the following two pathways can take place at low temperature. The first one is $C + H_2 \rightarrow HCH$ followed by $NH_3 + HCH + CO_2 \rightarrow$ glycine. The second one is $C + NH_3 \rightarrow CH_2NH$ followed by $CH_2NH + CO + H_2O \rightarrow$ glycine or $CH_2NH + CO_2 + H_2 \rightarrow$ glycine. The first pathway was also tested experimentally by adding C atoms to ice clusters containing H_2, NH_3, and CO_2 molecules. The detection of the main mass peak of glycine supported the feasibility of the proposed pathway.

Unified Astronomy Thesaurus concepts: Interstellar dust processes (838); Astrophysical dust processes (99); Prebiotic astrochemistry (2079); Astrochemistry (75); Astrobiology (74); Dark interstellar clouds (352)

1. Introduction

A large number of complex organic molecules (COMs) were detected in the gas phase in the interstellar medium (ISM; Hollis et al. 2000, 2006; Requena-Torres et al. 2008; Belloche et al. 2013; Cuppen et al. 2017). Many molecules are detected in the dense parts of the ISM, the temperature of which could be rather low, commonly reaching down to 10 K. Therefore, it is expected that larger organic molecules, including those which play a major role in biological processes (later, biological molecules), exist in the solid state in the ice mantel covering the refractory dust particles present in space. This is also in line with the observation of COMs in hot molecular cores, where the radiation from newly formed stars evaporates grain mantles (Nomura & Millar 2004). Further support comes also from analysis of meteoric materials delivered to Earth, which demonstrated the presence of amino acids, sugars, and nucleobases among other large COMs of extrasolar origin (Pizzarello & Cronin 1998; Ehrenfreund & Charnley 2000; Fray et al. 2016). The COMs can be transferred from the solid to the gas phase by shocks (Requena-Torres et al. 2008) or by simple UV irradiation, which is confirmed by the presence of glycine along with methylamine and ethylamine in the coma of the 67P/Churyumov–Gerasimenko comet (Altwegg et al. 2016). However, most biological molecules are impossible to transfer into the gas phase in such ways; instead, the destruction of the fragile molecules is expected. Moreover biological molecules are very fragile and can be easily destroyed in the harsh environment of the ISM (Pilling et al. 2008). Therefore, their abundances in the gas phase are expected to be low. As a result, there is not yet any convincing detection of glycine in the ISM. The presence of biological molecules in space attracts a lot of attention as their delivery to planets could facilitate the formation of the biopolymers and be the cause of the origin of life (Pearce et al. 2017).

The formation of dense clouds blocks most electromagnetic radiation and cools down all species. This leads to the conversion of the atomic gas present in the ISM into a molecular form. At the same time, all species accrete on the surface of refractory dust grains. Atoms are often very reactive and their rapid chemical reactions even at low temperatures lead to the formation of molecular ice mantels covering the refractory cores. The formed ice mantle is dominantly composed of the smallest molecules (H_2O, CO, CO_2, NH_3, and H_3COH), which can be easily formed due to reactions of the most abundant elements (Allamandola et al. 1999; Knez et al. 2008). However, C atoms are found to be highly reactive. In the gas phase and on the surface, they were found to react barrierlessly with a large variety of molecules (Kaiser et al. 1997; Bettinger et al. 2000; Walker & King 2000; Smith 2006; Shannon et al. 2014; Henning & Krasnokutski 2019; Krasnokutski et al. 2019a, 2017b, 2016). At the same time, atomic carbon is often found to be one of the most abundant carbonaceous species present even in the dense regions of the ISM (Schilke et al. 1995; Stark et al. 1996; Gerin et al. 1998). Therefore, the accretion of C atoms on the surface of grains is expected to generate a variety of large COMs. It is supported by condensation studies of C and H atoms, where the formation of a large variety of organic molecules was detected due to addition reactions of these atoms (Linnartz et al. 2015; Chuang et al. 2017; Krasnokutski et al. 2017a).

In the laboratory, glycine formation was found after energetic processing of different ices (Caro et al. 2002; Holtom et al. 2005; Elsila et al. 2007; Lee et al. 2009). Different pathways of the formation were suggested. The formation of the CN bond is of key importance in the formation of biological molecules. As a consequence, many suggested routes of glycine formation involve the HCN molecule, which has a high abundance in the ISM (Koch et al. 2008) and where the CN bond is already present. Alternatively, the reactions of

accreted C atoms can directly lead to the formation of CN bonds. For example, the C + NH_3 reaction in the gas phase was shown to lead to the formation of the H_2CN molecule (Bourgalais et al. 2015).

The main focus of the studies was always on the formation of the canonical form of glycine (NH_2CH_2COOH). At the same time, the zwitterionic form of glycine ($NH_3CH_2CO_2$) at which this molecule exists in crystals and in all living bodies could be of the same importance (Jonsson & Kvick 1972). Additionally, the interconversion between zwitterionic and canonical forms is very simple. For example, the evaporation of crystalline glycine leads to the formation of the canonical form of glycine in the gas phase (Junk & Svec 1963). Glycine has also a high conformational mobility (Huisken et al. 1999). Therefore, the interconversion between these two forms should also be efficient in the ISM. This zwitterionic form of glycine could be formed due to rather simple reactions between the abundant molecules NH_3, CH_2, and CO_2 present in the ISM. It becomes even more probable, as the CH_2 molecule can be formed due to the barrierless reaction C + H_2 → HCH on the surface of grains (Krasnokutski et al. 2016). The energy released in this reaction can help to overcome the energy barriers needed to join HCH with NH_3 and CO_2. Alternatively, several reaction routes were suggested based on computational results that lead to the formation of the canonical form of glycine starting with the HCH molecule, such as $NH_2 + CH_2 \rightarrow NH_2CH_2 + CO \rightarrow NH_2CH_2CO + OH \rightarrow NH_2CH_2COOH$ and $CH_2 + CO \rightarrow CH_2CO + OH \rightarrow CH_2COOH + NH_2 \rightarrow NH_2CH_2COOH$ (Singh et al. 2013). Additionally, barrierless reactions of singlet methylene ($^1CH_2$) with NH_3 and CO_2 molecules leading to the formation of glycine were predicted (Maeda & Ohno 2004).

In this study, we used experimental and computational approaches to test several pathways leading to the formation of glycine via C atom addition to a molecular ice, without the need of energetic processing of the ice. To have a better understanding of a possible chemistry process, the elementary reactions of C atoms with molecules present in ice mantels should be known. The reactions of C atoms with H_2 and CO_2 were reported in our previous works. We found barrierless reactions of C with H_2 leading to the formation of HCH (Krasnokutski et al. 2016; Henning & Krasnokutski 2019). Additionally, we found that at the interstellar conditions the C + CO_2 surface reaction will result in the formation of two CO molecules (Krasnokutski et al. 2019b). The study of the C + NH_3 reaction is present in this publication.

2. Experimental and Computational Methods

All experiments are performed in liquid helium droplets flying in vacuum. Liquid helium is a chemically neutral medium. It provides negligible influence on potential energy surfaces along which chemical reactions take place. Therefore, the energy level diagram of reactions occurring inside liquid helium is the same as for gas-phase reactions. The minor influence of liquid helium on the molecular energy levels is proven by the spectroscopic study of the species trapped in liquid helium, where the shift of electronic transitions is usually found to be below 100 cm^{-1} (Toennies & Vilesov 2004). At the same time, liquid helium serves as any other third body absorbing the reaction energy and preventing the fragmentation of the formed molecules. Therefore, all reactions between two species in liquid helium are similar to reactions of the same species occurring on a chemically inert surface. The water ice surface has as a rule a low catalytic activity, which leads to a moderate reduction of the reaction energy barriers (Rimola et al. 2014; Kobayashi et al. 2017; Lamberts & Kastner 2017). Although some specific small water clusters are found to provide a larger catalytic influence on the reaction involving hydrogen transport (Nhlabatsi et al. 2016a), they also lead to a reduction of the energy barriers. Therefore, we expect that those reactions that were found to be barrierless in helium droplets would also be barrierless on the surface of bulk water ice. Thus, the results of the He droplet studies provide guidance on reactions active on astrophysically relevant ices.

The He droplet apparatus is the same as that described in earlier publications (Krasnokutski & Huisken 2010, 2015). The gaseous helium (Westfalen AG, 99.9999% purity) was condensed into droplets during an adiabatic expansion of the compressed (20 Bar) gas into vacuum through a 5 μm pinhole nozzle. The nozzle temperature was kept constant equal to 11 K, resulting in helium droplets containing ∼15,000 helium atoms on average. The produced He droplets passed through the 0.3 mm diameter skimmer. In the next chamber, the He droplet beam was doped with reactants in the main 300 mm long chamber equipped with two different pick-up cells. The first pick-up cell was used to dope He droplets with gases, provided from outside through a leak valve. The H_2 and CO_2 are supplied either separately, or were premixed in the container before, the leak valve. The ammonia was supplied to the same pick-up cell always through a separate leak valve. The pressure in this pick-up cell is the same as in the main chamber, and was monitored by an ion gauges (Leybold Heraeus IE-20). Later, along the helium droplet beam path, the atomic carbon source was installed (Krasnokutski & Huisken 2014). The source was used to dope the helium droplets with ^{13}C atoms. The doping process as well as the purity of all reactants were controlled by a quadrupole mass spectrometer equipped with an electron impact ionization source (70 ev electron energy), which is installed in the last detector chamber. The same mass spectrometer was also used for the detection of glycine formation. The ionization of the dopants in helium droplets is different from that in the gas phase and is expected to happen in two steps. First, a He_2^+ molecule is formed due to the interaction of an electron and a helium droplet. On the next step, the charge is transferred to the dopant. However, the fragmentation pattern is about the same as in the case of direct electron impact ionization (Denifl et al. 2009). In particular, the mass spectrum of glycine recorded in our setup (Huisken et al. 1999) is very similar to the one from the NIST database (Linstrom & Mallard 2000).

The ultra-high vacuum (UHV) detector chamber is separated from the main pick-up chamber by an aperture of 800 μm diameter and a small differentially pumped vacuum chamber. This chamber is used to minimize the throughput of effusive gas to the UHV chamber. At the end, the He droplets evaporate after the collision with the walls of the UHV detector chamber. The gaseous helium is evacuated from this chamber at a constant speed. Therefore, the helium pressure in this chamber is proportional to the average size of arriving helium droplets (Krasnokutski & Huisken 2010). The pressure in this chamber was monitored with a precision ion gauge (Varian UHV-24). The pressure values are read by a computer at the times when the atomic C source was switched on (P_{ON}) and switched off (P_{OFF}). We estimate the change in size of helium droplets

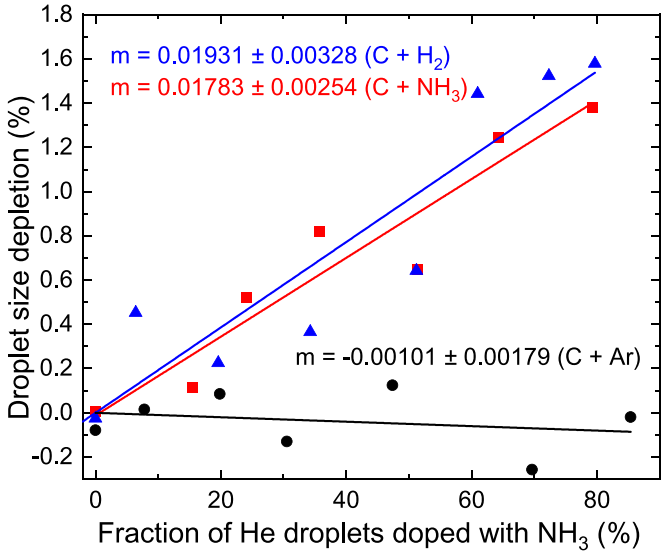

Figure 1. Depletion caused by the incorporation of C atoms into helium droplets as a function of the portion of helium droplets doped with a second reactant. The type of the second reactant is specified in the figure.

arriving in the detector chamber by the following equation $(P_{OFF}–P_{ON})/(P_{OFF}–P_{RES})$, where P_{RES} is the residual pressure in the detector chamber defined after 15 s of the complete block of the He droplet beam by the shutter in the source chamber. The on and off periods of the C source are equal to 30 s and 20 s gates were used for pressure averaging. The beginnings of gates were set eight seconds after the change of the condition of the C atom source.

Molecular geometries of possible products of chemical reactions between reactants were determined using the B3LYP hybrid functional and the 6-311+G (d, p) basis set implemented in the GAUSSIAN16 package (Frisch et al. 2009). The reaction energies (zero-kelvin enthalpies) were obtained as the difference between the sum of the energies of reactants and the energy of the product molecules with vibrational zero-point energy corrections. For a higher accuracy, the molecular structure of the most expected products were also optimized by the CCSD(T) method with the cc-pVQZ correlation consistent basis set. For the calculation of reaction energies, zero-point energy corrections were taken from DFT calculations. The two-dimensional potential energy scan of the CO_2 + HCH + NH_3 reaction was performed using the second-order Møller–Plesset perturbation energy (MP2) method and the 6-311+G (d, p) basis set. The MP2 method was selected for the scans due to its size consistency.

3. Results and Discussion

3.1. C + NH_3 Reaction

Figure 1 shows the calorimetry measurements of the C + NH_3 reaction. It demonstrates the reduction of average size of helium droplets caused by pick up of C atoms as a function of portion of the droplets doped with a second reactant. Here we used the C + H_2 and C + Ar reactions for the calibration of the calorimetry technique. The energy released in reactions is expected to be proportional to the measured slopes $E_R = K_{cal}m$, where K_{cal} is the calibration constant and m is the measured slope given in Figure 1 (Henning & Krasnokutski 2019). The energy released in the C + H_2 reaction (26,844 cm^{-1}) is precisely known, as can be derived based on

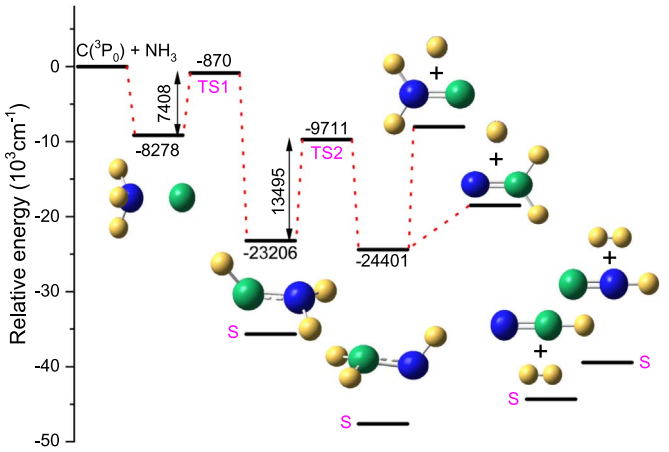

Figure 2. Energy level diagram of the C + NH_3 reaction and molecular structures of the products obtained in the b3lyp/6-311G+(d,p) level of computations. The numbers are energies obtained at the CCSD(T)/cc-pVQZ level of theory. Singlet and transition states are marked by S and TS correspondingly. The dashed line shows the most probable pathway of the chemical reaction.

Table 1
Energy Levels of the C + NH_3 Reaction Obtained from Quantum Chemical Computations Using (a) b3lyp/6-311G+(d,p) and (b) CCSD(T)/cc-pVQZ Levels of Theory

State	Energy[a] cm^{-1} (kJ mol^{-1})	Energy[b] cm^{-1} (kJ mol^{-1})
C ($^3P_0$) + NH_3	0	0
CNH_3	−9138, (−109)	−8278 (−99)
(TS1)	−2449 (−29)	−870 (−10)
$HCNH_2$	−24870 (−298)	−23206 (−278)
(S) $HCNH_2$	−35682 (−427)	
(TS2)	−11454 (−137)	−9711 (−116)
H_2CNH	−26700 (−319)	−24401 (−292)
(S) H_2CNH	−47618 (−570)	
CNH_2 + H	−8032 (−96)	
H_2CN + H	−18527 (−222)	
(S) CNH + H_2	−39432 (−472)	
(S) HCN + H_2	−44325 (−530)	

Note. Singlet and transition states are marked by (S) and (TS) correspondingly.

atomization energies of CH_2 and H_2 (Eyler & Melikechi 1993; Csaszar et al. 2003). The linear fit for the reaction of C with Ar shows a very small negative slope, which is due to the dissipation of the thermal energy of reactants during the pick-up process. This is in line with our previous measurements (Krasnokutski et al. 2019b). However, this effect is also present during the measurement of the calibration (C + H_2) reaction. Due to very similar slopes in the reactions of the C + H_2 and C + NH_3, this effect is properly included in the calibration and no additional corrections are required. Therefore, we can define the calibration constant to 1,390,161 cm^{-1} and correspondingly the energy released in the reaction of C + NH_3 to be equal to 24,787 ± 4500 cm^{-1}.

Figure 2 shows the energy level diagram for the reactions of C + NH_3 obtained in quantum chemical computations. The corresponding reaction energies are also summarized in Table 1. As can be seen, the most energy-favorable product of the reactions is the singlet state of H_2CNH. The formation of two singlet molecules, namely, the HCN and H_2 molecules, would result in the release of a comparable amount of energy.

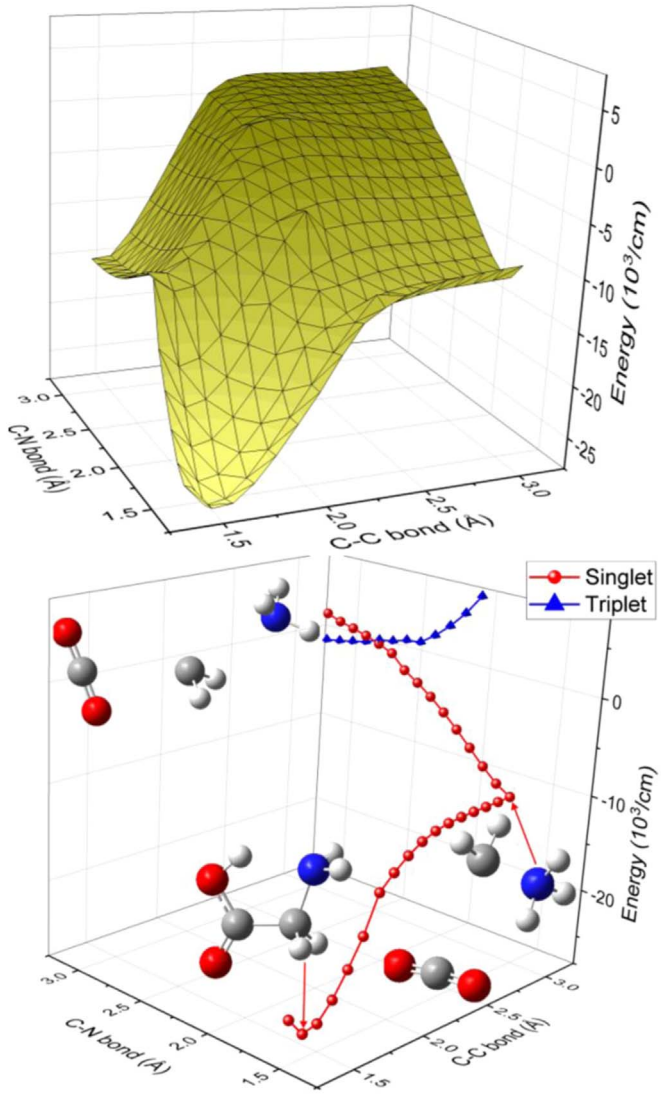

Figure 3. Potential energy surface of the singlet channel of the $CO_2 + CH_2 + NH_3$ reaction (top) and one of the barrierless pathways shown at the bottom. The molecular structures at different stages of the reaction are given.

This large amount of energy release that followed the formation of the singlet states is not compatible with the experimentally derived value. As the reaction starts with a triplet state, the formation of the most energy-favorable states requires an intersystem crossing but our results show a low probability of such a crossing. The comparison of the experimentally derived value with the DFT calculations suggests the formation of either H_2CNH or $HCNH_2$ molecules, which release nearly equal amounts of energy. These states were also optimized at the CCSD(T)/cc-pVQZ level of theory. The obtained values for the reaction energies are 24,401 and 23,206 cm^{-1}, correspondingly. The value of reaction energies associated with the formation of H_2CNH (24,401 cm^{-1}) better match with the experimentally derived value (24,787 cm^{-1}). However, considering uncertainties in the experimentally and computationally derived values, the formation of both H_2CNH and $HCNH_2$ molecules could be expected.

There are energy barriers to transfer protons from the nitrogen to the carbon side. The heights of barriers for the transfer of the first and the second protons are found to be 7408 cm^{-1} and 13,495 cm^{-1}, respectively. However, transition states are below the initial state, which correspond to the separated reactants. The transfer of the first proton to the carbon side is clearly evidenced from the comparison of computational and experimental values of reaction energies. This is in line with expectations as the excited state intramolecular proton transfer happens in a femtosecond timescale, while the time of thermal relaxation is in the order of picoseconds. (Chou et al. 2001; Lee et al. 2013). Therefore, in the formed exited molecule, the proton transfer takes place well before the product is cooled down. Consequently, we expect the transfer of both protons from the N to the C side and the formation of the most favorable triplet H_2CNH product in our experiments. Our results are in principal agreement with the previous study of this reaction in the gas phase, where the formation of the H + H_2CN products was found (Bourgalais et al. 2015).

3.2. The Glycine Formation

The formation of H_2CNH methylenimine is already an important step on the way to the formation of glycine. In several chemical pathways, suggested for the glycine formation in space, this molecule is an intermediate reactant (Koch et al. 2008; Singh et al. 2013; Nhlabatsi et al. 2016a, 2016b). The formation of glycine via the reactions of CH_2NH with the most abundant interstellar molecules seems to be the most relevant: (1) $CH_2NH + CO + H_2O \rightarrow$ glycine (energy barrier ~12,730), (2) $CH_2NH + CO_2 + H_2 \rightarrow$ glycine (energy barrier ~25,320 cm^{-1}). In both cases, in spite of the barrier in the reaction pathway obtained in the computations (B3LYP/6-31++G(d,p)), the low-temperature formation of glycine was predicted to be possible either via tunneling or due to the catalytic activity of other molecules present in ices (Nhlabatsi et al. 2016a, 2016b). The formation of CH_2NH molecules in the C + NH_3 reaction is followed by the release of a considerable amount of energy (24,787 cm^{-1}). These could help the reaction to overcome the existing energy barriers. What is even more important is that the CH_2NH molecule is formed in a long-living triplet state, which is about 23,217 cm^{-1} above the lowest energy singlet state. The reaction energy released in the reaction (24,787 cm^{-1}) is dissipated on a picosecond timescale, which could be faster compared with the time required for the reactions. At the same time, the lifetime of the triplet state is larger than one millisecond. Therefore, the energy stored in this excited state (23,217 cm^{-1}) can be used to activate the $CH_2NH + CO + H_2O \rightarrow$ glycine reaction.

Another simple pathway toward glycine involving molecules abundant in the ISM is the reaction $NH_3 + HCH + CO_2 \rightarrow$ glycine. In the case of the singlet CH_2, the reaction was predicted to be barrierless (Maeda & Ohno 2004). However, the lowest energy state of HCH is triplet and the lowest energy singlet state is about 3150 cm^{-1} above the triplet state (Shavitt 1985). Therefore, the abundance of the singlet HCH in low-temperature areas of the ISM should be quite low.

To better understand the possibility of such a reaction, we performed a two-dimensional scan over the potential energy surface of the reactions involving the reactants NH_3, HCH, and CO_2. In the scan, we varied the C–C distance between HCH and CO_2 and the C–N distance between HCH and NH_3 in a step of 0.1 Å. All other coordinates were relaxed and fully optimized at each step. We found indeed no energy barrier in the singlet channel of the glycine formation. However, when HCH is in the triplet state, the energy barrier for the transition

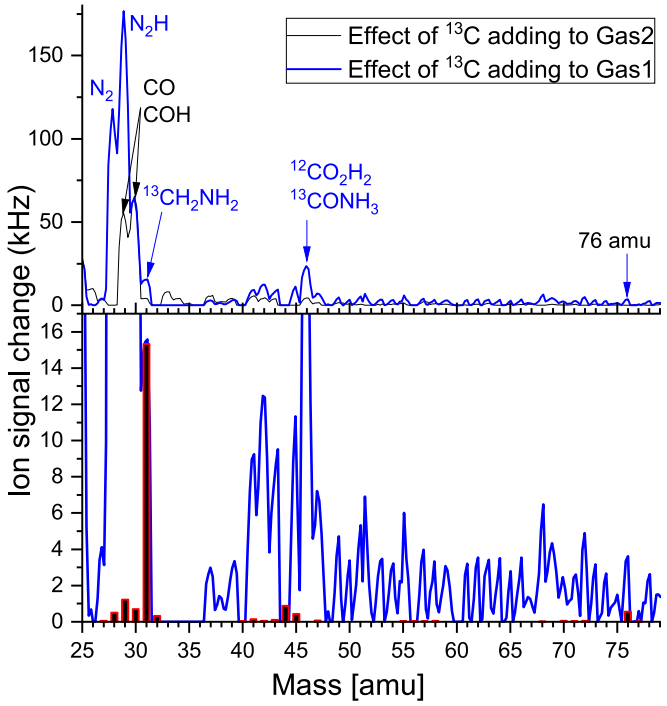

Figure 4. (a) Differential mass spectra showing the effect of the ^{13}C atom addition to the helium droplets containing ice clusters formed from different gases. (Gas 1—NH_3 50%, $H_2$33%, and $CO_2$17%; Gas 2—$H_2$65% and $CO_2$35%,). (b) The same mass spectrum as shown in panel (a) for Gas 1 in comparison with the glycine mass spectrum from the NIST database, which is shown by bars.

to the canonical form of glycine is found to be about 8000 cm^{-1}. Figure 3 shows one of the possible barrierless pathways for the reaction NH_3 + HCH + CO_2 → glycine in the singlet state. As can be seen from the figure, the lowest energy state for the separated reactants is the triplet. Therefore, such a reaction is not expected to be efficient at low temperatures. However, if the HCH molecule is formed due to the barrierless reaction of C atoms with H_2 molecules, the energy released in this reaction (~26,844 cm^{-1}) could help either to transfer the system into the singlet state or to help overcome the energy barrier present in the triplet reaction pathway. We also find a zero barrier for the transition between the canonical and the zwitterionic forms of glycine. The geometry optimization of the zwitterionic form results in the convergence to the canonical form.

This reaction pathway was also tested in our experiments. We first grow inside helium droplets an ice cluster by a sequent pick up of the H_2, CO_2, and NH_3 molecules. The aggregation of species picked up by helium droplets is expected to happen in a few microseconds (Loginov et al. 2011). Therefore, at the position where He droplets are doped with C atoms, the ice clusters are already formed. The products, which are formed due to the C addition to this ice, are monitored by mass spectrometry after electron impact ionization of the droplets. Figure 4 shows the differential mass spectra, which reflects the effect of ^{13}C atom addition to different ices. To obtain these mass spectra we recorded first the mass spectra of the helium droplets doped with pure ice clusters and later with the ice clusters with added ^{13}C atoms. In the differential mass spectra, all positive peaks show the new products formed in chemical reactions, while few negative peaks (not shown in the figure) belong to the reactants consumed in the reactions. To better visualize the formation of products involving nitrogen, we show two mass spectra with and without the presence of ammonia. The difference in these mass spectra clearly point to the products containing nitrogen. For example, it helps to identify the 46 amu peak, which can be assigned to both $^{12}CO_2H_2$ and $^{13}CONH_3$ molecules. As the intensity of this peak is weak without the presence of ammonia, the observed peak should be mainly caused by $^{13}CONH_3$ ions. We also clearly observe the formation of $^{13}CH_2NH_2$ ions, which are the main destruction products of the glycine molecules. Unfortunately, we were unable to clearly detect the formation of glycine ions with the mass of 76 amu. In this mass range, we observed an enhancement of the formation of the hydrogen helium clusters, which produce the mass peaks at almost each mass. We compared the obtained mass spectra with the mass spectrum of glycine from the NIST database. From this comparison we derived that the glycine signal at 76 amu should be much lower compared to the peaks observed in the recorded mass spectra. Moreover, almost the same peak intensities are observed for the masses of He_{17} and He_{18} clusters. Therefore, we conclude that the main signal on the mass 76 amu comes from He_{19}^+. This prevents the evaluation of the amount of the ions from undissociated glycine. In addition the ions with masses equal to reactants used in the experiment could not be detected as their amount decreased due to the consumption in the chemical reactions. Therefore, the differential mass spectra show only negative peaks at these masses. Another complication with the mass spectrometry detection is the occurrence of ion-molecular reactions after the ionization of the droplets. The importance of this chemistry is clearly evidenced by the presence of a large amount of N_2H, which cannot be formed in neutral–neutral reactions. In conclusion, the appearance of the main fragment of glycine in the differential mass spectrum point to a possible glycine formation. However, the mass peaks of additional ions produced in the experiments merge with other weak mass peaks of glycine preventing a firm identification.

3.3. Astrophysical Implications

In the ISM most of the carbon exists in the form of atomic gas, dominantly in C II form (Snow & Witt 1995). When the formation of dark molecular clouds takes place, the carbon is slowly converted to CO molecules C II → C I → CO. This conversion also takes place on edges of molecular clouds. When most of the carbon exists in C I form, the C atoms should also accrete on the surface of the dust, leading to an efficient formation of COMs and biological molecules on the surface. Fast low-temperature reactions of C atoms with almost all molecules present in the ice mantels in notable quantities were found (Kaiser et al. 1997; Wilson et al. 2012; Shannon et al. 2014; Bourgalais et al. 2015; Hickson et al. 2016; Krasnokutski et al. 2017a, 2017b, 2019b; Henning & Krasnokutski 2019). Due to this extremely high reactivity the accreted C atoms are expected to react with almost any molecule on the ice mantel via the Eley–Rideal mechanism. Therefore, the diffusion of reactants is not required. Such reactions should lead to the formation of a large variety of COMs. For example, just by including few surface reactions of C atoms to the chemical model Ruaud et al. (2015) managed to demonstrate a large abundance of COMs in the gas phase at temperatures as low as 10 K. The formation of COMs and hydrocarbon on the surface could also considerably contribute to the formation of CO molecules. Currently, the C II → C I → CO conversion is

considered to happen due to the gas-phase chemistry. It includes radioactive association steps for the formation of hydrocarbon molecules $C^+ + H_2 \rightarrow CH_2^+ + h\nu$. The following oxidation of hydrocarbons (CH_n) by atomic oxygen following decomposition of the formed products results in the formation of CO molecules (Wiebe et al. 2003). The surface reaction can therefore be very competitive for the formation of the hydrocarbon molecules ($C + H \rightarrow CH$ and $C + H_2 \rightarrow CH_2$) and additionally a considerable number of CO could be produced due to decomposition of COMs.

An interesting new possibility results from reactions involving several reactants, as was shown for the case of the reaction $NH_3 + HCH + CO_2 \rightarrow$ glycine in this study. Such reactions of multiple reactants are not usually considered in the chemical networks simulations. So-called three-body reactions, included in the chemical networks, consider the third body to be inert and only serving for the dissipation of reaction energy allowing associative reactions between two reactants (Rawlings et al. 2013; Potapov et al. 2017). However, if reactions take place on the surface or in the bulk, an appearing new radical can simultaneously react with two or even a larger number of molecules from ice. Such reactions could be particularly important for the formation of large molecules.

The other possibility, which is not commonly considered in the modern chemical models, is the reactions of hot products formed in other chemical reactions. In the case of gas-phase reactions, the time between collisions is long enough to allow a complete thermalization of the products before a second reaction can take place. However, in the case of surface reactions on ice, the hot products have a chance to react with neighboring molecules before the thermalization. This could help to overcome existing reaction barriers. The thermalization of the vibrationally hot molecules due to the interaction with environmental matter happens on a picosecond timescale (Sukowski et al. 1990). Therefore, the probability of chemical desorption is usually considered to be quite low (Ruaud et al. 2015). Our results demonstrate that some chemical processes like proton transfer could be much faster and therefore accomplished before the thermalization. However, the formation of reaction products in excited electronic states seems to be even more important. The relaxation of such excited states could be rather long. As was shown in our experiments, the reaction $C + NH_3$ leads to the formation of the $HNCH_2$ molecule in the excited triplet state. The lifetime of this excited state is longer than one millisecond, which corresponds to the duration of our experiment. Therefore, such excited products have enough time to participate in chemical reactions with neighboring molecules before the relaxation.

Including these processes in the chemical models should significantly enhance the efficiency of the COMs formation in particular in the case of large and biological molecules. A high reactivity of C atoms toward different molecules suggests the formation of a large variety of organic molecules that would be impossible to detect due to the low abundance of each individual species. Moreover, the detection of the molecules in the solid state is complicated. Abundances of only a few COMs were derived in the solid state (Schutte et al. 1996; Boogert et al. 2015). The amount of other COMs in the ice mantels was estimated based on the amount of COMs appearing in the gas-phase assumable due to nonthermal desorption in different astrophysical environments (Boogert et al. 2015; Cuadrado et al. 2017). However, the transfer of large molecules from the solid to the gas phase is often impossible. Therefore, we conclude that the amount of organic molecules in ice mantels could be significantly underestimated.

Our results demonstrated that the condensation of atomic species is likely to lead to the formation of glycine. The formation of other biological molecules may also be possible. This process is expected to be more important for the formation of biological molecules compared to the energetic processing of ices. The energetic processing destroys small molecules and forms reactive radicals, the reactions of which lead to the formation of COMs. However, energetic processing also results in the destruction of larger molecules. In the first instance, the fragile biomolecules are destroyed. The destruction of the organic commonly leads to the formation of pure carbon material and release of the other elements like O, H, etc., in the form of the smallest molecules (CO, CH_4, etc.). Therefore, the energetic formation pathway of any COM is counterbalanced by its photodestruction reaching a steady state (Stoker & Bullock 1997; Lee et al. 2009). At the same time, the condensation of atomic gas at low temperature does not have such restrictions. As is evidenced by our current results as well as by our previous work (Krasnokutski et al. 2017a), the condensation of atomic carbon at low temperature together with other species abundant in space leads mainly to the formation of organic molecules. In the case of low UV flux, they would not be destroyed and could cause a considerable fraction of organic molecules in the ice mantels. This is in line with the observation that most spectroscopically observed ice features are consistent with molecule formation on cold grain surfaces (Boogert et al. 2015). The COMs formation due to C atom addition is expected to take place in the low-temperature areas of the ISM, where refractory grains are covered by ice mantels. In this case, arriving C atoms react via the Eley–Rideal mechanism without the need to diffuse. Both C II and C I are expected to accrete on grains. The reactivity of C II is expected to be comparable to the reactivity of C I and additionally the fast C II → C I conversion is expected after the C II accretion due to the charge transfer. However, the importance of the C II for the COMs formation is expected to be lower due to the large fraction of the positively charged grains (Ibáñez-Mejıa et al. 2019). Additionally, the highest abundance of C II is in the zones where grains are not covered with ices and therefore, their accretion is expected to lead mostly to the formation of refractory carbon. At the same time, in the middle of dark clouds, the abundance of atomic carbon is decreasing as carbon is already converted into a molecular form. Therefore, the most efficient COMs formation is expected to take place in the translucent molecular clouds or on the edges of dense molecular clouds, where the density is $A_v \sim 1$–3 and the temperature range is about 15–80 K. However, the survival of the formed biomolecules in ices should be expected in the regions without intense UV flux.

4. Conclusion

The formation of glycine was suggested to proceed on the surface of ice mantels initiated by reactions of landed C atoms. The first pathway is initiated by the reaction $C + NH_3$. The quantum chemical calculations in combination with the experimental calorimetry method were applied to study this reaction. The reaction was found to be fast at $T = 0.37$ K leading to the formation of the H_2CNH product, which is in line with an extremely short time for the intramolecular proton

transfer. The formation of this molecule is followed by the release of 24,787 cm^{-1} of energy. The molecule is formed in the triplet state, which is about 21,000 cm^{-1} higher in energy compared to the most energy-favorable singlet state. The formed hot H_2CNH may further react with abundant molecules present in the ice mantels: $CH_2NH + CO + H_2O \rightarrow$ glycine and $CH_2NH + CO_2 + H_2 \rightarrow$ glycine. The other even more probable route of glycine formation is initiated by the reaction $C + H_2 \rightarrow HCH$. In our previous study, this reaction was found to be barrierless and released 26,844 cm^{-1} of energy. The reaction $NH_3 + HCH + CO_2 \rightarrow$ glycine has only a very small energy barrier in the triplet channel and is barrierless in the singlet state as revealed by our computations. Therefore, the reaction of the hot HCH molecule is very probable. In addition, the second pathway was also attempted to be tested experimentally adding C atoms to ice clusters containing H_2, NH_3, and CO_2 molecules. The detection of the main mass peak of glycine supported the feasibility of the proposed pathway. Unfortunately, due to the formation of a large variety of ions, the mass spectrometry technique cannot uniquely confirm the glycine formation. Further experiments are required.

The authors are grateful for the support by the Max Planck Institute for Astronomy (MPIA) and the Deutsche Forschungsgemeinschaft DFG (grant Nos. KR 3995/3-1, KR 3995/4-1). T.H. acknowledges support from the European Research Council under the Horizon 2020 Framework Program via the ERC Advanced Grant Origins 83 24 28.

ORCID iDs

Serge A. Krasnokutski https://orcid.org/0000-0002-9816-3187
Cornelia Jäger https://orcid.org/0000-0001-7803-0013

References

Allamandola, L. J., Bernstein, M. P., Sandford, S. A., & Walker, R. L. 1999, SSRv, 90, 219
Altwegg, K., Balsiger, H., Bar-Nun, A., et al. 2016, SciA, 2, e1600285
Belloche, A., Muller, H. S. P., Menten, K. M., et al. 2013, A&A, 559, A47
Bettinger, H. F., Schleyer, P. V., Schaefer, H. F., et al. 2000, JChPh, 113, 4250
Boogert, A. C. A., Gerakines, P. A., & Whittet, D. C. B. 2015, ARA&A, 53, 541
Bourgalais, J., Capron, M., Kailasanathan, R. K. A., et al. 2015, ApJ, 812, 106
Caro, G. M. M., Meierhenrich, U. J., Schutte, W. A., et al. 2002, Natur, 416, 403
Chou, P.-T., Chen, Y.-C., Yu, W.-S., et al. 2001, JPCA, 105, 1731
Chuang, K.-J., Fedoseev, G., Qasim, D., et al. 2017, MNRAS, 467, 2552
Csaszar, A. G., Leininger, M. L., & Szalay, V. 2003, JChPh, 118, 10631
Cuadrado, S., Goicoechea, J. R., Cernicharo, J., et al. 2017, A&A, 603, A124
Cuppen, H. M., Walsh, C., Lamberts, T., et al. 2017, SSRv, 212, 1
Denifl, S., Mahr, I., da Silva, F. F., et al. 2009, EPJD, 51, 73
Ehrenfreund, P., & Charnley, S. B. 2000, ARA&A, 38, 427
Elsila, J. E., Dworkin, J. P., Bernstein, M. P., et al. 2007, ApJ, 660, 911
Eyler, E. E., & Melikechi, N. 1993, PhRvA, 48, R18
Fray, N., Bardyn, A., Cottin, H., et al. 2016, Natur, 538, 72
Frisch, M. J., Trucks, G. W., Schlegel, H. B., et al. 2009, (Wallingford, CT: Gaussian, Inc)
Gerin, M., Phillips, T. G., Keene, J., et al. 1998, ApJ, 500, 329
Henning, T. K., & Krasnokutski, S. A. 2019, NatAs, 3, 568
Hickson, K. M., Loison, J. C., Nunez-Reyes, D., & Mereau, R. 2016, JPCL, 7, 3641
Hollis, J. M., Lovas, F. J., & Jewell, P. R. 2000, ApJL, 540, L107
Hollis, J. M., Remijan, A. J., Jewell, P. R., & Lovas, F. J. 2006, ApJ, 642, 933
Holtom, P. D., Bennett, C. J., Osamura, Y., et al. 2005, ApJ, 626, 940
Huisken, F., Werhahn, O., Ivanov, A. Y., & Krasnokutski, S. A. 1999, JChPh, 111, 2978
Ibáñez-Mejıa, J. C., Walch, S., Ivlev, A. V., et al. 2019, MNRAS, 485, 1220
Jonsson, P. G., & Kvick, A. 1972, Acta Crystallogr. B, B, 28, 1827
Junk, G., & Svec, H. 1963, JACS, 85, 839
Kaiser, R. I., Ochsenfeld, C., Head-Gordon, M., et al. 1997, JChPh, 106, 1729
Knez, C., Moore, M., Travis, S., et al. 2008, IAU Symp. 251, Organic Matter in Space, 47ed. S. Kwok & S. A. Sanford, (Cambridge: Cambridge Univ. Press)
Kobayashi, H., Hidaka, H., Lamberts, T., et al. 2017, ApJ, 837, 155
Koch, D. M., Toubin, C., Peslherbe, G. H., & Hynes, J. T. 2008, JPCc, 112, 2972
Krasnokutski, S. A., Goulart, M., Gordon, E. B., et al. 2017a, ApJ, 847, 89
Krasnokutski, S. A., Gruenewald, M., Jäger, C., et al. 2019a, ApJ, 874, 149
Krasnokutski, S. A., & Huisken, F. 2010, JPCa, 114, 13045
Krasnokutski, S. A., & Huisken, F. 2014, ApPhL, 105, 113506
Krasnokutski, S. A., & Huisken, F. 2015, JChPh, 142, 084311
Krasnokutski, S. A., Huisken, F., Jäger, C., & Henning, T. 2017b, ApJ, 836, 32
Krasnokutski, S. A., Kuhn, M., Renzler, M., et al. 2016, ApJL, 818, L31
Krasnokutski, S. A., Tkachenko, O., Jäger, C., & Henning, T. 2019b, PCCP, 21, 12986
Lamberts, T., & Kastner, J. 2017, ApJ, 846, 43
Lee, C. W., Kim, J. K., Moon, E. S., et al. 2009, ApJ, 697, 428
Lee, J., Kim, C. H., & Joo, T. 2013, JPCA, 117, 1400
Linnartz, H., Ioppolo, S., & Fedoseev, G. 2015, IRPC, 34, 205
Linstrom, P. J., & Mallard, W. G. (ed.) 2000, NIST Chemistry WebBook, NIST Standard Reference Database Number 69 (Gaithersburg MD: NIST), 20899, https://doi.org/10.18434/T4D303
Loginov, E., Gomez, L. F., Chiang, N., et al. 2011, PhRvL, 106, 233401
Maeda, S., & Ohno, K. 2004, CPL, 398, 240
Nhlabatsi, Z. P., Bhasi, P., & Sitha, S. 2016a, PCCP, 18, 375
Nhlabatsi, Z. P., Bhasi, P., & Sitha, S. 2016b, PCCP, 18, 20109
Nomura, H., & Millar, T. J. 2004, A&A, 414, 409
Pearce, B. K. D., Pudritz, R. E., Semenov, D. A., & Henning, T. K. 2017, PNAS, 114, 11327
Pilling, S., Andrade, D. P. P., de Castilho, R. B., et al. 2008, in IAU Symp. 251, Organic Matter in Space (Cambridge: Cambridge University Press), 371ed. S. Kwok & S. A. Sanford
Pizzarello, S., & Cronin, J. R. 1998, Natur, 394, 236
Potapov, A., Canosa, A., Jiménez, E., & Rowe, B. 2017, Angew. Chem. Int. Ed., 56, 8618
Rawlings, J. M. C., Williams, D. A., Viti, S., & Cecchi-Pestellini, C. 2013, MNRAS, 436, L59
Requena-Torres, M. A., Martin-Pintado, J., Martin, S., & Morris, M. R. 2008, ApJ, 672, 352
Rimola, A., Taquet, V., Ugliengo, P., et al. 2014, A&A, 572, A70
Ruaud, M., Loison, J. C., Hickson, K. M., et al. 2015, MNRAS, 447, 4004
Schilke, P., Keene, J., Lebourlot, J., et al. 1995, A&A, 294, L17
Schutte, W. A., Gerakines, P. A., Geballe, T. R., et al. 1996, A&A, 309, 633
Shannon, R. J., Cossou, C., Loison, J. C., et al. 2014, Rsc Advances, 4, 26342
Shavitt, I. 1985, Tetrahedron, 41, 1531
Singh, A., Shivani, M. A., & Tandon, P. 2013, RAA, 13, 912
Smith, I. W. M. 2006, Angew. Chem. Int. Ed., 45, 2842
Snow, T. P., & Witt, A. N. 1995, Sci, 270, 1455
Stark, R., Wesselius, P. R., vanDishoeck, E. F., & Laureijs, R. J. 1996, A&A, 311, 282
Stoker, C. R., & Bullock, M. A. 1997, JGR, 102, 10881
Sukowski, U., Seilmeier, A., Elsaesser, T., & Fischer, S. F. 1990, JChPh, 93, 4094
Toennies, J. P., & Vilesov, A. F. 2004, Angew. Chem. Int. Ed., 43, 2622
Walker, A. V., & King, D. A. 2000, JChPh, 112, 1937
Wiebe, D., Semenov, D., & Henning, T. 2003, A&A, 399, 197
Wilson, A. V., Parker, D. S. N., Zhang, F. T., & Kaiser, R. I. 2012, PCCP, 14, 477